Journal of Hydrology 512 (2014) 421–434

Contents lists available at ScienceDirect

Journal of Hydrology

journal homepage: www.elsevier.com/locate/jhydrol

Identification of changes in hydrological drought characteristics from a multi-GCM driven ensemble constrained by observed discharge

M.H.J. van Huijgevoort *, H.A.J. van Lanen, A.J. Teuling, R. Uijlenhoet

Hydrology and Quantitative Water Management Group, Wageningen University, PO Box 47, 6700 AA Wageningen, The Netherlands

ARTICLE INFO

Article history:
Received 20 December 2013
Received in revised form 20 February 2014
Accepted 22 February 2014
Available online 13 March 2014
This manuscript was handled by Konstantine P. Georgakakos, Editor-in-Chief, with the assistance of Ashish Sharma, Associate Editor

Keywords:
Hydrological drought
River discharge
Global scale
Climate change
Multi-model

SUMMARY

Drought severity and related socio-economic impacts are expected to increase due to climate change. To better adapt to these impacts, more knowledge on changes in future hydrological drought characteristics (e.g. frequency, duration) is needed rather than only knowledge on changes in meteorological or soil moisture drought characteristics. In this study, effects of climate change on droughts in several river basins across the globe were investigated. Downscaled and bias-corrected data from three General Circulation Models (GCMs) for the A2 emission scenario were used as forcing for large-scale models. Results from five large-scale hydrological models (GHMs) run within the EU-WATCH project were used to identify low flows and hydrological drought characteristics in the control period (1971–2000) and the future period (2071–2100). Low flows were defined by the monthly 20th percentile from discharge (Q20). The variable threshold level method was applied to determine hydrological drought characteristics. The climatology of normalized Q20 from model results for the control period was compared with the climatology of normalized Q20 from observed discharge of the Global Runoff Data Centre. An observation-constrained selection of model combinations (GHM and GCM) was made based on this comparison. Prior to the assessment of future change, the selected model combinations were evaluated against observations in the period 2001–2010 for a number of river basins. The majority of the combinations (82%) that performed sufficiently in the control period, also performed sufficiently in the period 2001–2010. With the selected model combinations, future changes in drought for each river basin were identified. In cold climates, model combinations projected a regime shift and increase in low flows between the control period and future period. Arid climates were found to become even drier in the future by all model combinations. Agreement between the combinations on future low flows was low in humid climates. Changes in hydrological drought characteristics relative to the control period did not correspond to changes in low flows in all river basins. In most basins (around 65%), drought duration and deficit were projected to increase by the majority of the selected model combinations, while a decrease in low flows was projected in less basins (around 51%). Even if low discharge (monthly Q20) was not projected to decrease for each month, droughts became more severe, for example in some basins in cold climates. This is partly caused by the use of the threshold of the control period to determine drought events in the future, which led to unintended droughts in terms of expected impacts. It is important to consider both low discharge and hydrological drought characteristics to anticipate on changes in droughts for implementation of correct adaptation measures to safeguard future water resources.

1. Introduction

Drought events and their related impacts on society and environment are expected to increase in severity due to changing climate (e.g. Bates et al., 2008; Dai, 2011; Romm, 2011). Droughts occur across the world in all climatic regions and are still difficult to quantify (Wilhite, 2000; Tallaksen and van Lanen, 2004; Mishra and Singh, 2010). Drought remains one of the natural hazards for which predictions are most uncertain. Many studies have investigated the effect of climate change on discharge regimes (e.g. Arnell, 1999; Nijssen et al., 2001a; Manabe et al., 2004; Milly et al., 2005; Nohara et al., 2006; Sperna Weiland et al., 2012). Besides investigating changes in the regime, low flows are included in some studies as well (e.g. Arnell and Gosling, 2013). The main conclusions about the expected changes are in agreement. For example, the discharge is expected to increase in cold climates and a shift of the snow melt peak in these areas is projected (e.g. Sperna Weiland

* Corresponding author. Tel.: +31 (0)317 481511.
E-mail address: Marjolein.vanHuijgevoort@wur.nl (M.H.J. van Huijgevoort).

http://dx.doi.org/10.1016/j.jhydrol.2014.02.060
0022-1694/© 2014 The Authors. Published by Elsevier B.V.

et al., 2012). In addition to the impact of climate change on discharge, effects on drought have been investigated. In the 21st century, drought may intensify in parts of Europe, central North America, Central America and Mexico, northeast Brazil and southern Africa (Seneviratne et al., 2012). Studies on drought in the future have mainly focused on soil moisture (e.g. Sheffield and Wood, 2008; Vidal et al., 2012; Dai, 2013; Orlowsky and Seneviratne, 2013). A decrease in soil moisture was detected at the global scale by Sheffield and Wood (2008), leading to more soil moisture drought events. Vidal et al. (2012) found that all characteristics of soil moisture or agricultural drought events in France increased in the 21st century. Severe drought conditions in the 21st century over large parts of the globe were determined with the PDSI by Dai (2013). A large range in soil moisture drought projections at global scale was found by Orlowsky and Seneviratne (2013), but increased drought was consistent in several regions, namely the Mediterranean, South Africa and Central America/Mexico. Less is known about changes in hydrological drought events (drought in groundwater and surface water). Hirabayashi et al. (2008) have studied changes in number of drought days at the global scale by taking the annual drought days from discharge data. Significant increases in drought were found for many regions across the globe (Hirabayashi et al., 2008). For Europe, Feyen and Dankers (2009) investigated changes in streamflow drought by deriving low flows and drought deficits. They concluded that in many rivers, with the exception of rivers in the most northern and northeastern parts of Europe, minimum river flows and flow deficit volumes became more severe in the frost-free season. Most studies on changes in discharge are carried out at the catchment scale instead of the global scale. For example, Madadgar and Moradkhani (2013) used trivariate copulas to determine changes in drought characteristics for a specific catchment in Oregon. They concluded that drought events will become less severe in the future in this catchment. Knowledge on hydrological drought events is important for water resources and needed for adequate planning and assessment of drought impacts in the future. This knowledge across the globe is rather limited.

In recent years, more and more gridded models have been developed for hydrological studies at the global scale. However, many scenario studies employ only one global hydrological model (GHM) in combination with one or an ensemble of General Circulation Models (GCMs) that provide forcing data (e.g. Sperna Weiland et al., 2012; Arnell and Gosling, 2013). Because GHMs can show large differences in the representation of runoff for the previous century (e.g. Gudmundsson et al., 2012; Van Huijgevoort et al., 2013), including multiple GHMs for future analysis is important. This was also concluded by Hagemann et al. (2013), who used 8 GHMs and 3 GCMs to analyse water resources and found that spread in hydrological models in some regions is larger than that of climate models. They recommend that analyses of global climate change impacts should use results from multiple impact (hydrological) models.

To reduce or to better adapt to the impacts of hydrological drought across the globe, more knowledge regarding changes in hydrological drought characteristics (e.g. frequency, duration) in the future is needed in addition to already existing knowledge regarding changes in meteorological and soil moisture drought. In this study, effects of a climate change scenario on drought in several river basins across the globe with contrasting climates and catchment characteristics were investigated using a multi-model analysis. The aim of this study is to investigate changes in both low flows and drought events, and to illustrate the challenges associated with this kind of drought analysis. Results of five GHMs forced with three GCMs have been used for the analysis over two periods, the control period (1971–2000) and future period (2071–2100). As a first step towards reducing the range of projected changes in drought, model combinations (GHM and GCM) have been constrained for analysis in the future period through comparison with observed discharge in the control period. Monthly low discharge values from selected model combinations for the control period and future period and changes therein have been determined. Changes in hydrological drought characteristics relative to the control period were identified from the selected model combinations using the variable threshold level method.

2. Data

2.1. Observed river discharge

From the Global Runoff Data Centre (GRDC, 2013) discharge data were available for selected river basins across the globe. The locations of the discharge gauges of these 41 selected (sub)basins are given in Fig. 1. Table 1 gives an overview with the names of the rivers, abbreviations, locations of gauging stations, periods of data used for comparison with large-scale models and the basin areas. The selection of the river basins was based on the following criteria:

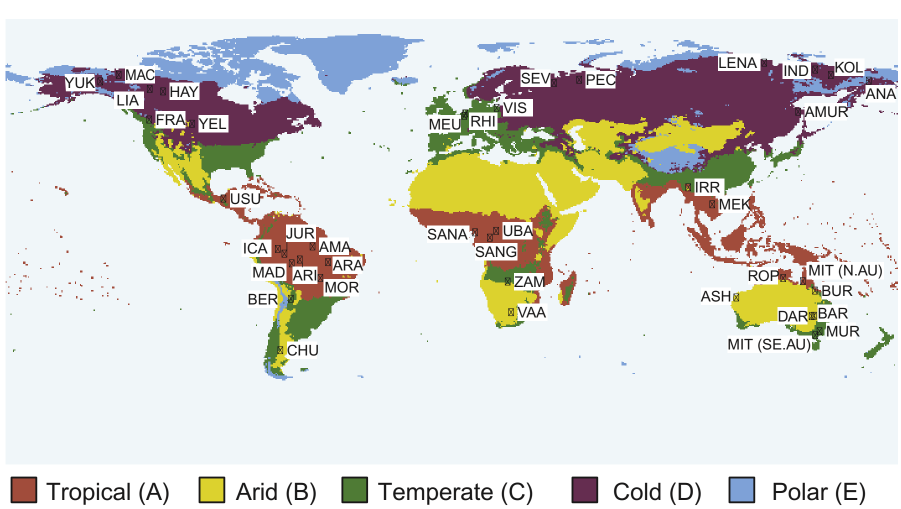

Fig. 1. Location of the gauging station for each river basin in the major climate zones (see Table 1 for river basin abbreviations).

Table 1
Information about the selected river basins.

River	Abbreviation	Longitude[a]	Latitude[a]	Period	Area (* 10^3 km^2)
Vaal[b]	VAA	24.60	−28.50	1971–2000	121
Zambezi	ZAM	23.25	−16.12	1971–2000	285
Sanaga	SANA	10.07	3.77	1971–1980	132
Sangha	SANG	16.05	1.62	1971–1983	158
Ubangi[c]	UBA	18.58	4.37	1971–2007	500
Ashburton	ASH	115.50	−22.54	1972–2000	71
Roper[c]	ROP	134.42	−14.70	1971–2010	47
Mitchell (N Au)[c]	MIT (N.AU)	142.38	−15.95	1972–2010	46
Burdekin[c]	BUR	147.24	−19.76	1971–2010	130
Barwon (Trib. Darling, Murray)	BAR	146.87	−29.95	1971–2000	298
Darling[b]	DAR	145.94	−30.09	1971–2000	386
Murrumbidgee	MUR	149.09	−36.16	1971–2000	1.9
Mitchell (Se Au)[c]	MIT (SE.AU)	147.37	−37.76	1971–2010	3.9
Irrawaddy	IRR	96.10	21.98	1978–1988	118
Mekong	MEK	105.80	15.12	1971–1993	545
Usumacinta	USU	−91.48	17.43	1971–2000	48
Içá	ICA	−69.52	−2.94	1973–1993	108
Jurua[c]	JUR	−66.85	−4.84	1972–2010	162
Madeira	MAD	−63.92	−8.75	1971–2000	976
Aripuana[c]	ARI	−60.65	−7.21	1974–2010	131
Amazon	AMA	−55.51	−1.92	1971–2000	4680
Araguaia	ARA	−49.26	−8.27	1971–2000	320
Rio Das Mortes[b]	MOR	−52.36	−14.67	1971–2000	25
Bermejo	BER	−64.22	−23.10	1971–1980	25
Chubut	CHU	−68.50	−43.85	1971–1994	16
Meuse[c]	MEU	5.72	50.87	1971–2010	21
Rhine[b,c]	RHI	6.11	51.84	1971–2010	161
Vistula (Wisla)	VIS	18.80	54.10	1971–1994	194
Yellowstone[c]	YEL	−104.16	47.68	1971–2010	179
Fraser[c]	FRA	−121.45	49.38	1971–2010	217
Hay[c]	HAY	−115.86	60.74	1971–2010	52
Liard[c]	LIA	−121.22	61.75	1972–2010	275
Yukon[c]	YUK	−141.20	64.79	1971–2010	294
Mackenzie[c]	MAC	−133.74	67.46	1972–2010	1660
Amur	AMUR	140.47	52.53	1971–1987	1790
Anadyr	ANA	169.00	65.08	1971–1988	47
Kolyma	KOL	153.67	67.37	1971–2000	361
Indigirka	IND	147.35	69.58	1971–1998	305
Lena	LENA	126.80	72.37	1971–2000	2460
Pechora	PEC	52.10	65.45	1971–1998	248
Severnaya Dvina (Northern Dvina)	SEV	41.92	64.15	1971–2000	348

[a] Coordinates of gauging station.
[b] River basins not included in the analysis of the future period, because none of the model combinations reached the criterion (Section 3).
[c] River basins used to evaluate the selection criterion.

1. The basins should be located in as many climate zones as possible (Fig. 1). Climate zones are based on the Köppen–Geiger classification (Peel et al., 2007) of the WATCH forcing data, see Wanders et al. (2010). The five major climate types are the equatorial (A), arid (B), warm temperature (C), snow (D), and polar climates (E).
2. The length of available discharge time series was important, because for drought analysis long time series are needed. Preferably time series were at least 30 years long and covered the control period (1971–2000, Section 2.2). However, to include all climate zones, ten river basins with shorter time series (less than 25 years) were also selected as a compromise. A number of river basins was used to evaluate the methodology for selecting model combinations (Section 3) in the period 2001–2010.
3. Basin area should include enough grid cells of the large-scale models to make a comparison.
4. Since naturalized runs of the large-scale models were used, the basins should be as undisturbed as possible in terms of human influences, like dams.

The selection of the basins is somewhat biased to the northern colder climates, because more streamflow records were available there and reservoir storage is less important than in warmer, drier climates (Nijssen et al., 2001b).

2.2. Forcing data

In this study, we used model output from runs with three different GCMs for the SRES A2 scenario (Nakićenović and Swart, 2000). The A2 scenario was chosen to investigate the most extreme changes in drought events. The three GCMs, made available through the European WATCH project (Water and Global Change, www.eu-watch.org), were: ECHAM5/MPIOM of the Max Planck Institute for Meteorology (Jungclaus et al., 2006), CNRM-CM3 of the National Centre for Meteorological Research (Royer et al., 2002; Salas Mélia, 2002) and IPSL-CM4 of the Institute Pierre Simon Laplace (Hourdin et al., 2006; Fichefet and Morales Maqueda, 1997; Goosse and Fichefet, 1999). The three GCMs chosen within WATCH belong to different model families and partly cover the range from the CMIP3 ensemble in projected precipitation change (Masson and Knutti, 2011). In an assessment of GCM skill in simulating persistence by Johnson et al. (2011), all three chosen GCMs were ranked among the best performing models for their skill in predicting global precipitation, sea surface temperature and surface pressure.

Bias-corrected forcing data were available from 1960 to 2100. We have taken the period 1971–2000 as the control period and 2071–2100 as the future period. A shorter period 2001–2010 was used to evaluate our methodology for selecting model combinations

(Section 3) in a number of river basins (Table 1). All GCM output was downscaled to 0.5° and was bias corrected with the WATCH forcing data (Weedon et al., 2011) for rainfall, snowfall, and minimum, mean and maximum air temperature. The procedure for the statistical bias correction of GCM output is described by Piani et al. (2010), Chen et al. (2011), Haerter et al. (2011) and Hagemann et al. (2011). The WATCH forcing data consist of gridded time series of meteorological variables for 1958–2001 and originate from modification (bias-correction and downscaling) of the ECMWF ERA-40 re-analysis data (Weedon et al., 2011).

Fig. 2 gives the difference in precipitation for the three GCMs between the control period and the future period. Largest differences in mean daily precipitation are given by IPSL. For some regions all GCMs agree on the direction of change, for example a decrease in precipitation in Central America, southern Europe and parts of Australia. Other regions have changes that differ for each GCM, for example in the Amazon region. For temperature, all GCMs indicate an increase across the globe, although the magnitude of the increase differs (not shown).

2.3. Large-scale hydrological models

Results from 5 different gridded large-scale hydrological models were made available through the WATCH project. The models

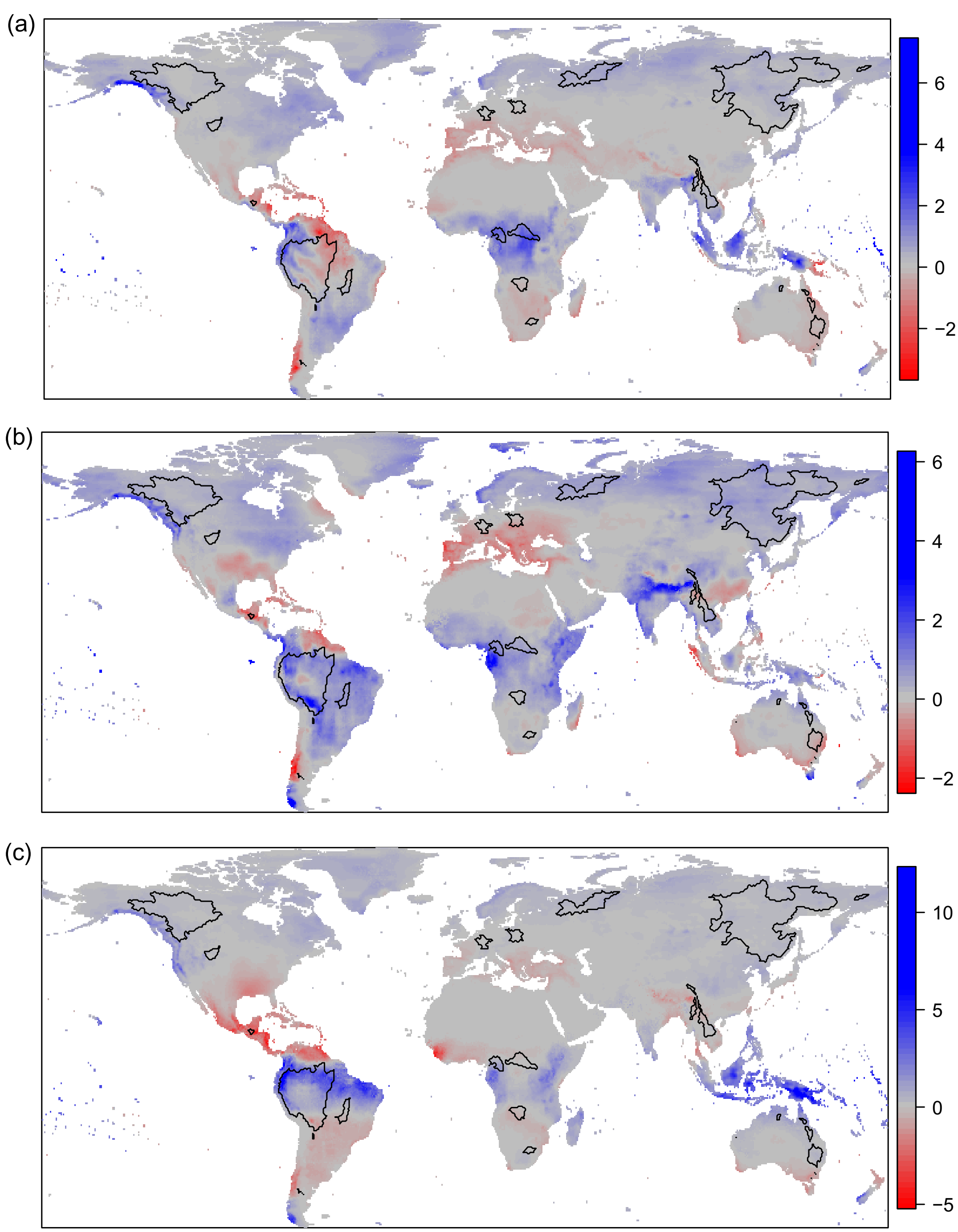

Fig. 2. Difference between future period (2071–2100) and control period (1971–2001) in mean daily precipitation (mm day^{-1}) for three GCMs (a: ECHAM5, b: CNRM, c: IPSL) for the A2 scenario. River basins are indicated with black polygons.

used in this study are: Jules, LPJml, MPI, Watergap and Orchidee. They all have a resolution of $0.5^{\circ} \times 0.5^{\circ}$. All models are run with the same forcing data for the period 1960–2100 (Section 2.2) and have the same routing network. The main characteristics of the models and references are given in Table 2, more information can be found in Haddeland et al. (2011).

Daily time series of discharge were used in this study to focus on low flows and hydrological drought, and to be able to compare the model results with observations. Time series of routed discharge were taken from the grid cell in which the gauging stations are located. Discharge values consist of spatially aggregated gridded total runoff (sum of surface and subsurface runoff) from the grid cells in the models that represent the basin. Total runoff has been routed with the same network in each model.

3. Low flow and drought identification

The forcing data for the models is obtained from GCMs. These GCMs do not reproduce time series of historical weather in the control period, but the average climate conditions. This implies that time series of modelled discharge and observed discharge cannot directly be compared either. Therefore, as a measure of low flows, the 20th percentile (Q20) for each month was calculated, which is defined as the value that is equalled or exceeded 80% of the time, for observed discharge and simulated discharge. When comparing the climatology of Q20 values of the simulated discharges against observations, there was a large difference in absolute values for most basins. The large differences between observations and model results can have different causes, for example, weaknesses in climate forcing, model structure and observations, and has been found in previous studies, e.g. Sperna Weiland et al. (2010). Because drought events were derived from anomalies, all monthly Q20 values were normalized by dividing the Q20 values by the yearly mean,

$$Q20^{*}(i) = Q20(i)/\overline{Q20}, \tag{1}$$

where i is month of the year. This way the models could be judged on their ability to simulate the regime, which is important for drought analysis.

A selection has been made from the 15 model combinations (GHM and GCM) for analysis in the future based on the Nash–Sutcliffe coefficient (Nash and Sutcliffe, 1970) between the climatology of $Q20^{*}$ of observed discharge and the climatology of $Q20^{*}$ of simulated discharge in the control period. A value of 1 indicates a perfect match between model results and observations, while a value below 0 indicates that taking the observed mean is a better predictor than the model results. All model combinations with a Nash–Sutcliffe coefficient of 0.4 or higher were used for analysis of future drought. The criterion of 0.4 is rather arbitrary, but it was chosen based on visual inspection of the climatology of $Q20^{*}$ for simulated discharges and to keep as many as possible model combinations in the future analysis.

To analyse hydrological drought events and determine drought characteristics, the variable threshold level method (e.g. Yevjevich, 1967; Hisdal et al., 2004) was used. The start of a drought event is indicated by the point in time when discharge falls below the threshold and the event continues until the threshold is exceeded again. A monthly threshold derived from the 20th percentile of the time series was applied in this study. The discrete monthly threshold values were smoothed by applying a centred moving average of 30 days (Van Loon and Van Lanen, 2012). Drought characteristics derived in this study are the number of drought events, the average duration of drought events and the standardized mean deficit volume (Hisdal et al., 2004; Van Lanen et al., 2013). Due to the definition of the standardized mean deficit volume (deficit volume divided by the mean discharge), it has unit 'day', which indicates the number of days that mean flow is missing. To identify changes in drought events between the control period and the future period, droughts were determined with the same threshold, based on the control period.

4. Results and discussion

4.1. Comparison of large-scale models and observations

The climatologies of $Q20^{*}$ from the model combinations (GHM and GCM) were compared with the observed $Q20^{*}$ climatology. A selection of model combinations was made based on a Nash–Sutcliffe efficiency (NSE) above 0.4 for the control period. Fig. 3 shows the model combinations that met this criterion for each river with at least one combination selected. After this selection 37 river basins were left (Table 1). Clearly, the number of model combinations and the selected combinations were different for each river basin (Fig. 3). The range of all 15 model combinations is also given in Fig. 3. In all rivers, the range was reduced by the selection, except for the Meuse river for which all model combinations had a NSE above 0.4. In most river basins, the hydrological model had more influence on the simulation than the GCM (e.g. Murrumbidgee river with selected combinations 3a, 3b, 3c, 4a, 4b, 4c; Chubut river with combinations 3a, 3b, 3c, 5b; Madeira river with combinations 1a, 1b, 1c, 3a, 3b, 3c, 4b, 5a, 5b, 5c). In most river basins, the selection of model combinations included one or multiple GHMs with all three GCMs. So forcing was less important than the hydrological

Table 2
Main characteristics of the selected models (derived from Haddeland et al., 2011).

No.	Model name	Model timestep	Meteorological forcing variables[a]	Energy balance	Evapotranspiration scheme[b]	Runoff scheme[c]	Snow scheme	Reference(s)
1	JULES	1 h	R, S, T, W, Q, LW, SW, SP	Yes	Penman-Monteith	Infiltration excess/ Darcy	Energy balance	Best et al. (2011) and Clark et al. (2011)
2	LPJmL	Daily	P, T, LWn, SW	No	Priestley-Taylor	Saturation excess	Degree day	Bondeau et al. (2007) and Rost et al. (2008)
3	MPI-HM	Daily	P, T	No	Thornthwaite	Saturation excess/ Beta function	Degree day	Hagemann and Gates (2003) and Hagemann and Dümenil (1998)
4	WaterGAP	Daily	P, T, LWn, SW	No	Priestley-Taylor	Beta function	Degree day	Alcamo et al. (2003)
5	Orchidee	15 min	R, S, T, W, Q, SW, LW, SP	Yes	Bulk formula	Saturation excess	Energy balance	De Rosnay and Polcher (1998)

[a] R: Rainfall rate, S: Snowfall rate, P: Precipitation (rain or snow distinguished in the model), T: air temperature, W: Wind speed, Q: Specific humidity, LW: Longwave radiation flux (downward), LWn: Longwave radiation flux (net), SW: Shortwave radiation flux (downward), SP: Surface pressure.
[b] Bulk formula: Bulk transfer coefficients are used when calculating the turbulent heat fluxes.
[c] Beta function: Runoff is a nonlinear function of soil moisture.

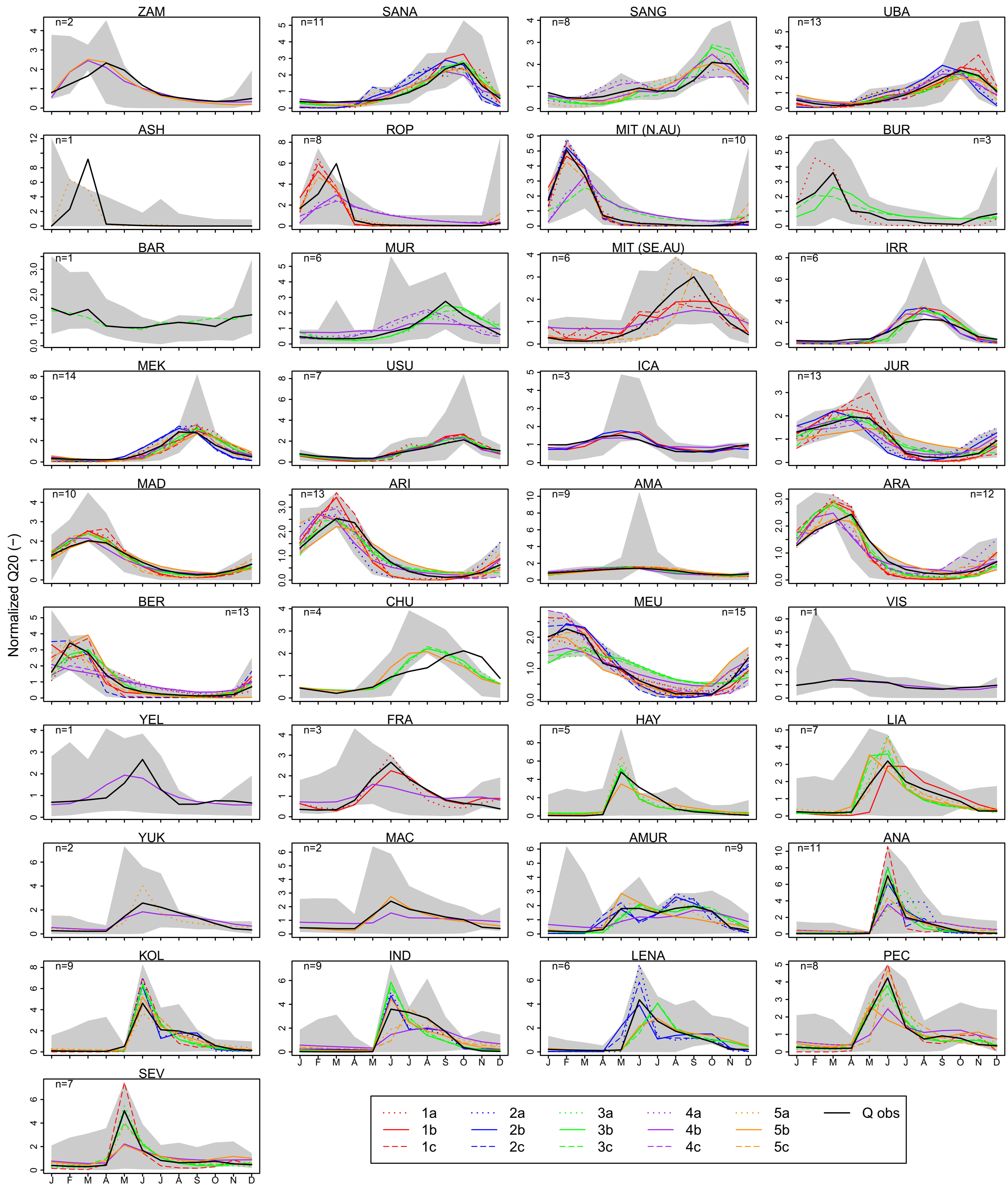

Fig. 3. Climatology of normalized Q20 values of simulated discharge and observed discharge (Q obs). Model combinations (GHM and GCM) shown are selected for analysis of future drought (number of combinations is given by *n*), the grey areas indicate the range of all 15 model combinations. The number indicated in the legend refers to the hydrological model (Table 2), the character to the GCM (a: ECHAM5, b: CNRM, and c: IPSL).

model, which supports the findings of Hagemann et al. (2013). However, there are also river basins in which the simulations were dominated by the choice of the GCM (e.g. Içá river with combinations 1b, 2b, 4b; Mackenzie river with combinations 4b, 5b; Zambezi river with combinations 4b, 5b).

The number of model combinations left for further analysis depended on the NSE value used for the selection. Fig. 4 shows how the number of selected models decreased with increasing NSE values (averaged over all basins). Based on this analysis, we adopted 0.4 as the selection criterion. A NSE of 0.4 is generally accepted

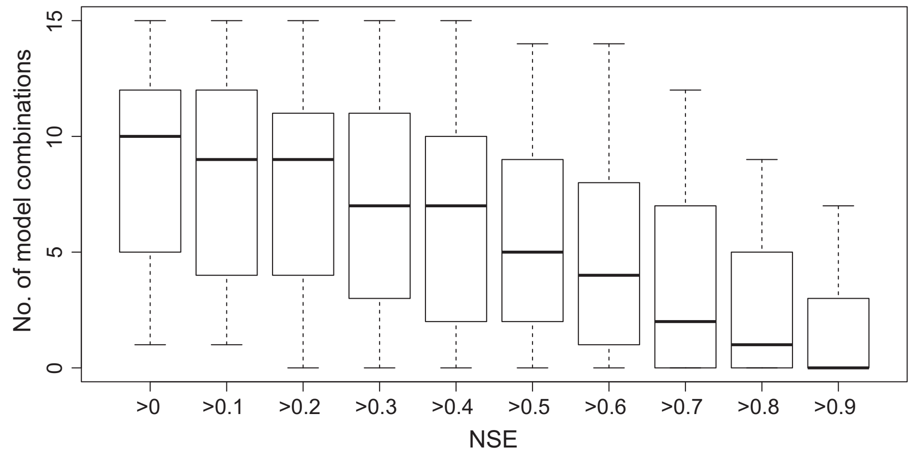

Fig. 4. Number of model combinations selected based on different Nash–Sutcliffe efficiencies.

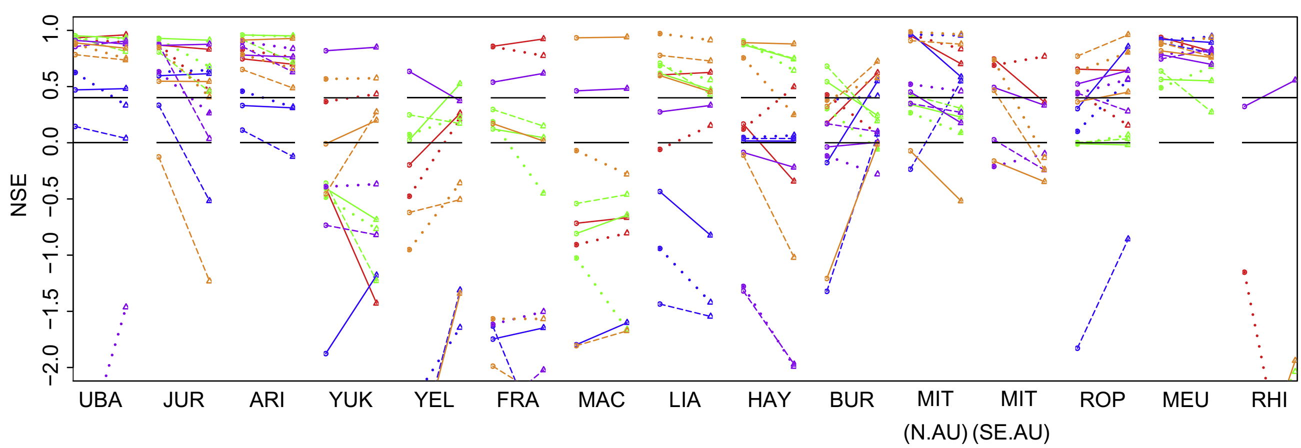

Fig. 5. Direction of change in Nash–Sutcliffe efficiency for a subset of river basins between period 1971–2000 (p1, circle) and period 2001–2010 (p2, triangle). See Table 1 for exceptions in data availability in these periods for some river basins. Black horizontal lines indicate NSE values of 0 and 0.4 (the selection criterion). Other colours and line styles are similar to Fig. 3.

to reflect a reasonable model performance, while with higher NSE values, the number of model combinations quickly dropped. By using the criterion of 0.4, the median of the model combinations left was 7 across all river basins.

The selection of GHM and GCM combinations has been made to reduce the range, and thereby uncertainty, in projections. Previous studies have argued not to make a selection of the models or a ranking, because information could get lost (e.g. Gosling et al., 2011). Furthermore, it has been argued that results based on historical information might not determine model performance in the future (Reifen and Toumi, 2009). However, other studies (Hall and Qu, 2006; Stegehuis et al., 2013) have shown that if GCMs are constrained with observations, the uncertainty in the future is reduced. We believe that in order to achieve projections of future hydrological drought to determine the effects on water resources, a reduction of the large range in model projections is necessary. Some model combinations resulted in negative NSE even for the $Q20^*$ climatology, which means that even the regimes of the rivers were not modelled correctly. It is questionable if these model combinations could give any useful information about future changes in discharge in these rivers. The selection made in this study is subjective in terms of selecting the NSE as criterion and the magnitude of the NSE. It should be considered as a first step towards a methodology to reduce the range in future hydrological drought. Other additional criteria to select models could be included in the methodology.

To investigate the robustness of the assumption that model combinations with a very low NSE should be excluded, the NSE was also calculated for a subset of rivers (Table 1) for the period 2001–2010. This period was not used in the comparison of GCM output and forcing data to derive the bias-correction method (Section 2.2) and can thus be regarded as near future relative to the control period. Since the period 2001–2010 is too short to validate the models properly, this period was only used to provide a preliminary test of the robustness of the selection method. Observed data were not available for a longer period. Fig. 5 gives the NSE values for the river basins with available observed data for two periods, 1971–2000 (p1) and 2001–2010 (p2). Overall, the NSE values are reasonably constant, i.e. the majority of the combinations with a NSE value above 0.4 in the control period also gave a NSE value above 0.4 in the following period (82%). This means that only 18% of the model combinations with a value above 0.4 in the control period dropped below 0.4 in the next period. Only two model combinations with NSE above 0.4 in the control period dropped below a NSE of zero (both for the Mitchell river (Se Au), combinations 5a and 5c). Model combinations with a very low NSE value (even below −2) did not recover in the following period. Although the threshold choice (NSE = 0.4) is arbitrary,

Fig. 5 indicates that performance in the past can provide an indication for the future.

Clearly, it is difficult to judge the effect of selecting only models that perform well in the control period given that all projections are uncertain. Nevertheless we believe that models that perform better against observations, have a higher plausibility and the range in the projected changes can be reduced. However, river basins with only one or a few selected model combinations left, need to be investigated more in detail, since such a small selection might not be representative (Hagemann et al., 2013). For these specific river basins with a limited number of model combinations, other hydrological models with a different structure or model runs including human influence might be better suited. Although river basins were selected to be as undisturbed as possible, because the model results did not take into account human influence, it was difficult to find completely undisturbed basins in some regions and therefore human influence might be larger than expected. To analyse climate change in these specific river basins a detailed analysis is needed, which is beyond the scope of this study. The selection of the model combinations is determined by the chosen criterion. For specific basins other criteria might be more suitable. More research is needed to determine additional criteria for the selection of suitable model combinations.

Besides additional criteria for the selection of suitable model combinations, another option would be to keep all model combinations, but use a model averaging method instead. For the selection made in this study, model results below a certain NSE value are removed from the analysis for the future. When using an averaging method, all model results are taken into account. By using Bayesian model averaging (BMA), model results with a better performance are given larger weights in the ensemble average (Duan et al., 2007). Different ways to implement the BMA are described by Parrish et al. (2012). The BMA method was applied by Najafi et al. (2011) to assess uncertainties of hydrological model selection in a climate change impact study for a specific catchment. They found that the BMA allowed for quantifying model structure uncertainties and performing ensemble estimation. However, they also mention that models with poor performances may reduce the performance of the BMA and removing poor results increases the performance of the BMA (Najafi et al., 2011). This may indicate that a combination of selection of models based on certain criteria and a model averaging method is the most promising way to assess climate change impact.

We realize that the employed models are not completely independent of each other. All GCMs or all GHMs describe the same system and will therefore have common elements (Masson and Knutti, 2011). The model combinations used in this study include three GCMs and five GHMs. The three GCMs belong to different model families (Masson and Knutti, 2011). The GHM selection contains land surface models as well as global hydrological models (Haddeland et al., 2011). The model structures show differences and the different forcing variables used by each of the models give some indication about the different parameterizations in the models (Table 2). By using a range of GCMs and GHMs the dependence between the models was limited. However, it is impossible to make a model selection that is completely independent given the fact that all models have to simulate the same processes. It is important to use a multi-model ensemble for climate change assessments to encompass different model structures and parameterizations.

4.2. Influence of climate change on low flows

To investigate the influence of climate change, the difference between the climatology of Q20 (monthly Q20 values derived from model results) in the future period and the climatology of Q20 (monthly Q20 values derived from model results) in the control period was calculated for all river basins for the selected model combinations (Fig. 6). The agreement between the model combinations on the changes is indicated in Fig. 6 by the intensity of the colours. There was no overall consistent drying or wetting trend in all selected rivers across the globe. The number of selected model combinations that agreed on the direction of change in low discharges differed between the river basins (ranging from 50% to 100% for the mean of the monthly changes in Q20, from now indicated as mean change Q20). In most major climate zones, however, the direction of changes in low discharges for the river basins was largely similar. In the arid climates, models tended to agree on a decrease in the low discharge. For example, the Murrumbidgee river and the Mitchell river (Se Au, third row in Fig. 6) for which all models agreed on negative mean change Q20 (i.e. will become drier). Also rivers on the border of the arid climate zone, like the Zambezi river and the Chubut river, showed a decrease in low discharge. For other rivers at this border, the Roper river and the Mitchell river (N Au), changes were less uniform (around 50% of the models agreed on the direction of mean change Q20). Models did not all agree on increase or decrease of low discharges in these basins. The projected changes in low discharge corresponded with the changes in precipitation (Fig. 2). Precipitation decreased in southern Australia, the Zambezi river basin and Chubut river basin, while increases or no changes were obtained for northern Australia.

For rivers located mainly in tropical (A) climates, models disagreed on the changes, although this differed per continent. All rivers in the humid climates in Africa (Sanaga, Sangha and Ubangi, first row in Fig. 6) and most rivers in the Amazon region (Jurua, Madeira, Aripuana, Amazon and Araguaia, fourth and fifth row in Fig. 6) showed changes in low discharges in both directions, and thus it was difficult to predict changes in drying or wetting for these regions (model agreement on the direction of mean change Q20 was between 50% and 75%). For the river basins in Africa, the GCMs indicated an increase or no change in precipitation. This is not directly visible in low discharge changes because of other processes that determine discharge as well, e.g. changes in evapotranspiration and storage. This highlights the importance of using hydrological models for hydrological drought analysis instead of only GCMs which generally have a more crude land surface model component. For the Amazon region, changes in precipitation were not uniform among the GCMs and again other hydrological processes affect discharge changes. One exception regarding low discharge changes in the Amazon region was the Içá river. For this river all selected model combinations indicated an increase in low discharge for the months April to July, followed by a decrease in low discharge. For the Içá river, the selection of model combinations resulted in only one GCM (CNRM, Fig. 3), which could explain the uniform changes in discharge. Other rivers in humid climates (Irrawaddy, Mekong and Usumacinta, third and fourth row in Fig. 6) showed a decrease in low discharge for most models for the whole year or at least a large part of the year (all models agreed on a negative mean change Q20). For the Usumacinta river, however, all GCMs projected a large decrease in precipitation, which translated in a decrease in low discharge. For the Mekong river and Irrawaddy river projected precipitation changes were less uniform.

There were almost no rivers in the selection in temperate climates (Fig. 1), partly because rivers in these regions were often largely affected and partly because model performance was poor for these rivers. For the Meuse river, most models gave an increased low discharge in winter and decreased low discharge in summer. This means that the low discharges in wet periods became higher and in dry periods became lower, as was the case for the Içá river. The Bermejo river is on the border of climate zones

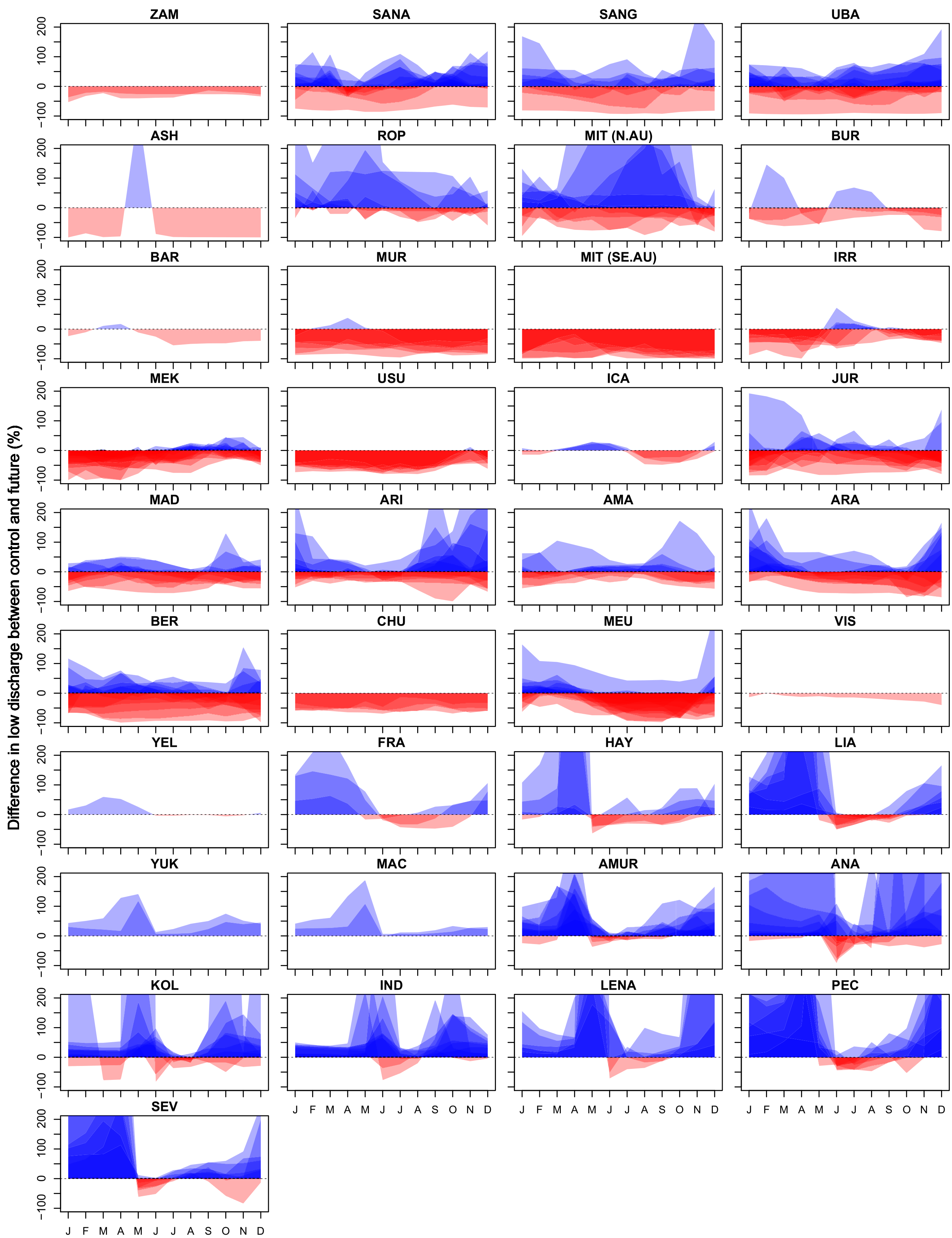

Fig. 6. Relative change in low flows (Q20) between future period (2071–2100) and control period (1971–2000) given as percentage of low discharge in the control period. Red indicates a decrease in Q20 in the future period, blue indicates an increase in Q20. All selected model combinations (GHM and GCM) for each river basin are shown. The darker the colour, the more models have the same difference.

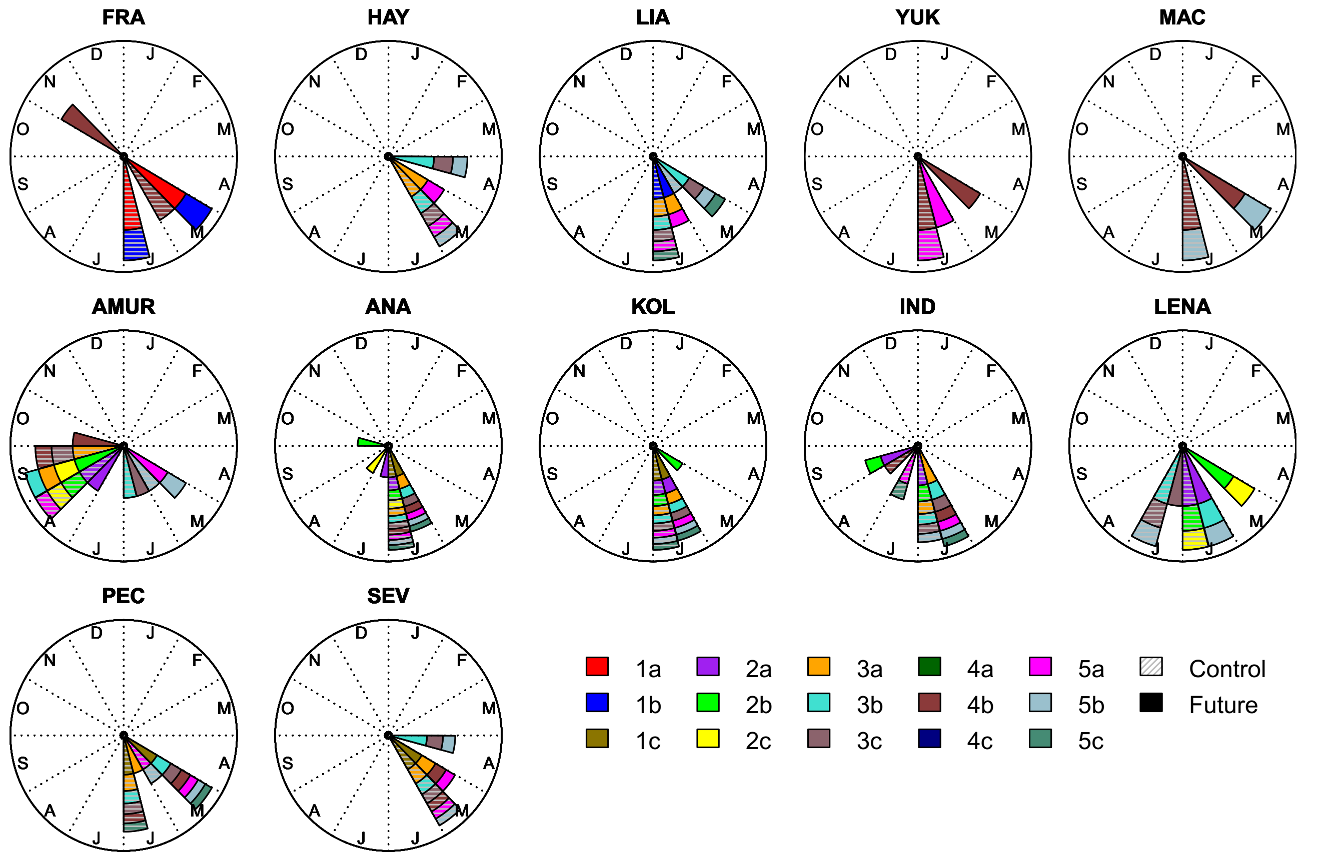

Fig. 7. Timing of the seasonal peak in Q20 between the control period (shaded colours) and the future period (full colours) given for all river basins in cold climates that showed differences for the selected model combinations (GHM and GCM). (The length of the radius of the segments is determined by the number of selected model combinations and has no additional meaning.)

(Fig. 1) and showed differences in low discharges in both directions and little model agreement, which was triggered by the GCMs that disagreed on precipitation change.

Changes in river discharges in the cold climates (D and E, bottom four rows in Fig. 6) were dominated by a shift in the regime caused by an earlier snow melt peak and less snowfall due to higher temperatures. The mean yearly low discharge (mean Q20) in these rivers increased according to most models. The change in timing of the snow melt peak is shown in Fig. 7, where the month with the highest Q20 value in the year is given for both the control period and the future period for each model combination. In most river basins, there is only 1 month difference between the models for the timing of the peak. Not for all rivers in cold climates a change in the timing of the snow melt peak was predicted by the models (e.g. Kolyma river, Anadyr river). However, in some cases models agreed that the snow melt peak would occur one month earlier in the future (e.g. Lena river, MacKenzie river, Pechora river).

An overview of previous studies on the change in runoff or discharge caused by climate change is given by Sperna Weiland et al. (2012). Their overview mentions regions found to be affected either by an increase or a decrease of discharge or runoff. Although most previous studies focused on mean discharge and not on low flows, we have compared our results with their findings here by lack of studies on low streamflow at the global scale. The shift in regime in northern colder river basins and the increase in low discharge found in this study corresponded well with results on discharge changes from e.g. Arnell and Gosling (2013), Sperna Weiland et al. (2012), Nohara et al. (2006) and Milly et al. (2005). Also our findings that arid river basins will become drier in the future corresponded well with previous studies (e.g. Tang and Lettenmaier, 2012; Nohara et al., 2006; Sperna Weiland et al., 2012; Milly et al., 2005). Changes in low discharge for the rivers in the Amazon region were less certain in this study. There was less agreement with previous studies and these previous studies disagree on changes. Arnell (2003), Arnell and Gosling (2013) and Arora and Boer (2001) found a decrease in discharge or runoff in this region, while Nijssen et al. (2001a), Manabe et al. (2004) and Nohara et al. (2006) found an increase in mean annual discharge for the Amazon. The decrease of low discharges during large parts of the year in the Asian rivers, Irrawaddy and Mekong, found here is not in agreement with all other studies (e.g. Nijssen et al., 2001a; Sperna Weiland et al., 2012), which showed an increase in discharge for the Mekong, although Manabe et al. (2004) and Arora and Boer (2001) also found a decrease for the Mekong. Changes in low discharge found for the Meuse river in this study correspond with findings of De Wit et al. (2007) that seasonality in the discharge regime of the Meuse will be enhanced. However, they also stated that groundwater storage is important in the Meuse basin and a decrease in mean summer discharge might not necessarily lead to more severe low flows. Differences between climate change studies and the current study are caused by a different focus of the studies (e.g. mean discharge instead of low flows) and the use of different hydrological models, climate models and emission scenarios.

4.3. Influence of climate change on hydrological drought characteristics

With the variable threshold level method (Section 3), drought events and their characteristics have been determined for the

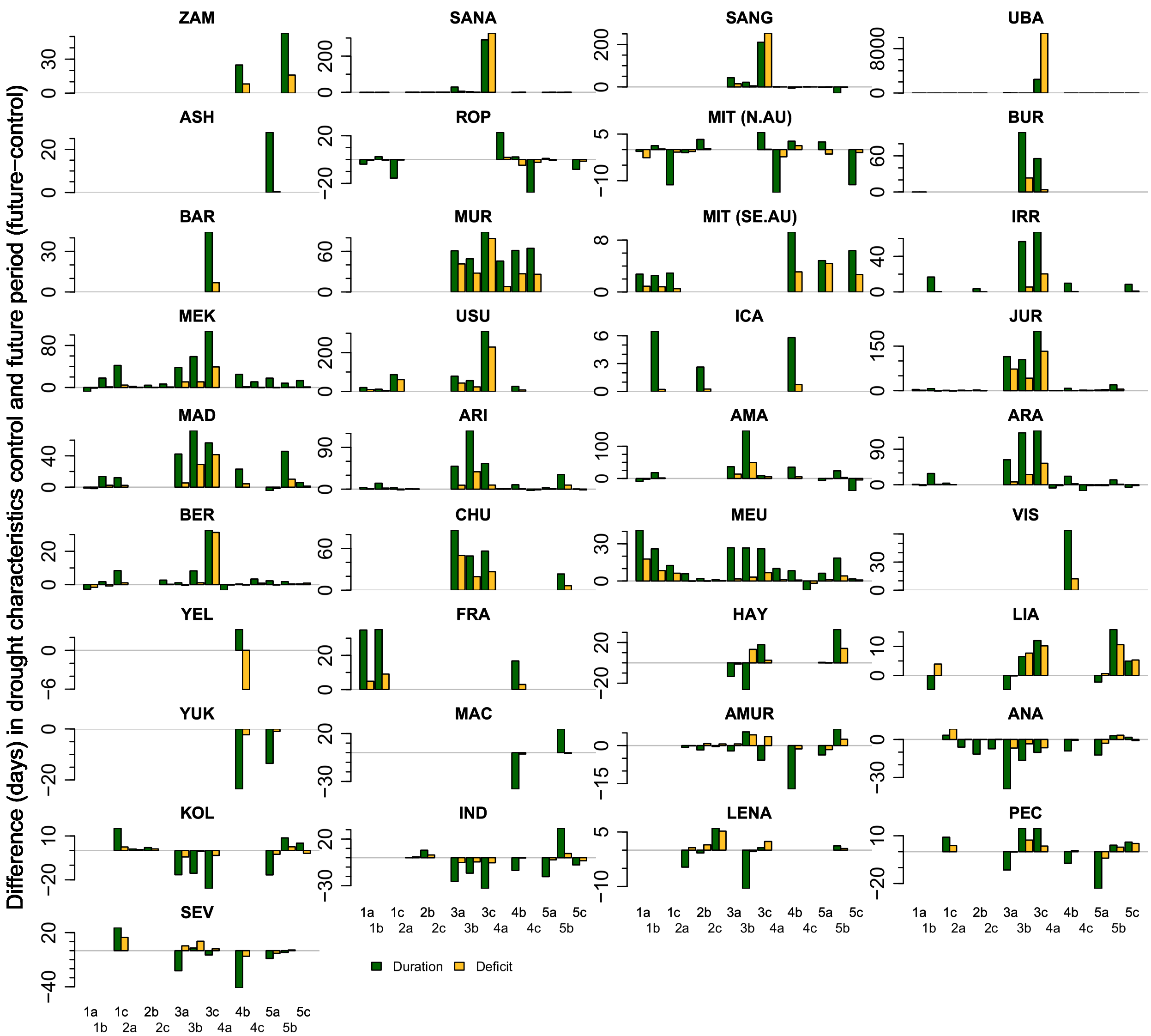

Fig. 8. Change in drought characteristics (mean duration and mean standardized deficit volume) between future period (2071–2100) and control period (1971–2000) for the selected combinations of GCM and GHM. Codes for the combinations are equal to Fig. 3. Positive change means longer droughts or higher standardized deficit volumes in the future, whereas negative change means the opposite.

control period and the future period. The changes in drought characteristics, mean drought duration and standardized deficit volume, between the future period and the control period are shown in Fig. 8 for each river basin. It was expected that when model combinations projected a decrease in low discharges, drought characteristics would show an increase. In general, differences in hydrological drought characteristics (Fig. 8) showed the same pattern as the differences in Q20 (Fig. 6). In river basins with a high model agreement for changes in Q20, drought characteristics also showed high agreement and followed the direction of change in Q20 with a negative correlation as expected. For example, all model combinations showed an increase in drought duration and standardized deficit volume for the Usumacinta river (USU, Fig. 8), which also showed a decrease in low discharge (Fig. 6). The rivers in arid regions (Murrumbidgee and Mitchell (Se Au)) also showed a decrease in low discharge and this resulted in an increase in drought characteristics. Especially in these dry regions this could have large impacts, since there is already little water available.

There was higher model agreement on differences in drought characteristics than on changes of the climatology of Q20 in other river basins, e.g. Madeira river, Jurua river, Amazon river. For these rivers, both drought characteristics showed an increase (Fig. 8), while the model combinations did not agree on a clear increase or decrease for the Q20 discharge (Fig. 6). This means severity and impact of drought events will likely increase in these basins, although uncertainty in changes of low discharge was large.

For the Meuse river and Içá river, the model combinations projected seasonality in low discharges would become more extreme (Fig. 6). The drought analysis showed that the increase in seasonality led to an increase in both drought characteristics for almost all selected model combinations. So, even though Q20 values were higher during the wet period, drought duration increased and drought impacts will be more severe in the future because of the decrease in summer discharge.

In some river basins in cold climates that showed a clear snow melt peak, there were model combinations that gave an opposite signal in drought characteristics as compared to the signal in discharge, e.g. the Liard river and the Fraser river. The overall Q20 discharge in these basins seemed to increase (Fig. 6), whereas the drought duration and standardized deficit volume also increased (Fig. 8). This was partly caused by the application of the threshold

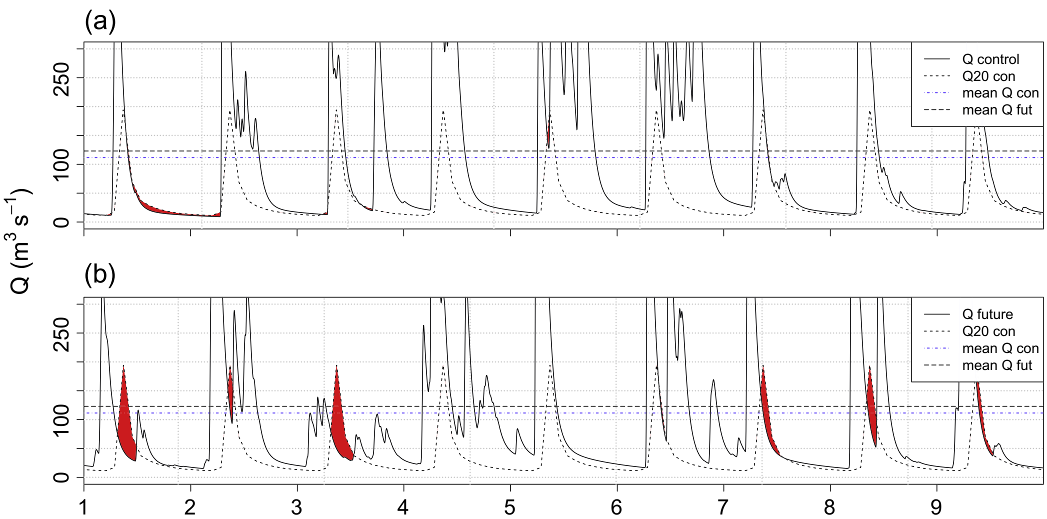

Fig. 9. Influence of a threshold derived from the control period on identification of drought events (red polygons) in the future in case of a regime shift: (a) drought events identified from simulated discharge in the control period, (b) drought events identified from simulated discharge in the future period.

level method to the future period using a threshold derived from the control period (Fig. 9). In case of a shift in the timing of the snow melt peak in the Q20 values, anomalies in discharge behind the peak could be inadvertently identified as drought (in terms of expected impacts), even though the mean discharge increases from the control period to the future period. However, the increase in drought characteristics was also caused by a decrease of summer discharge as projected by some model combinations (Fig. 6). In that case, the number of summer droughts will increase in these regions even if mean discharge increases. Adaptation measures to prevent large impacts of these summer droughts will be necessary.

Fig. 9 indicates that it is not straightforward to determine hydrological drought events with the variable threshold method using the same threshold both in the control period and in the future period. The use of the threshold derived from the control period can lead to unintended drought events in terms of expected impacts. The natural variability of the climate over 100 years is not taken into account and it is difficult to determine the impact of drought events in the future, because possible adaptation to the changing conditions could occur. This adaptation could be included by linking the drought threshold to adaptation scenarios like Vidal et al. (2012). This would require more information to formulate accurate scenarios, but could be an important step in future hydrological drought identification studies. Drought identification in the future is very dependent on the identification method used and should include both drought characteristics and low flows to indicate changes. If only low flows are considered, effects on drought events in the future could be underestimated, for example as seen in the rivers in the Amazon region (Figs. 6 and 8).

The differences in low flows and drought characteristics between the control and future period found in this study are based on model runs that do not include adaptation policies. In that way they should be seen as a guidance to assess if measures are necessary. An important factor that is missing in the hydrological models is change in vegetation. The hydrological models, except for LPJmL, do not include vegetation changes or take into account the response of stomata to increased CO_2 (Lammertsma et al., 2011). This stomatal adaptation is believed to affect evapotranspiration and thus runoff (Field et al., 1995), although evidence for this effect on evapotranspiration is questionable (Huntington, 2008), also questioning the possible effect of stomatal adaptation on future drought. Prudhomme et al. (2013) have concluded that vegetation change will affect drought characteristics in the future, but the magnitude of the effect remains uncertain. In this study, no clear difference between the changes in drought for the LPJmL model and the other models was found. More research is needed to quantify the effect of vegetation change on drought in the future. This also confirms that it is important to use multiple GHMs in climate change studies to include effects that may not be represented by all models.

5. Conclusions

For adequate adaptation to the impacts of hydrological drought events, robust predictions about changes in their characteristics in the future is important. In the current study, an ensemble of Global Hydrological Models (GHMs) forced with different General Circulation Models (GCMs) was used to analyse low flows and drought events. To reduce the range in future drought projections, a selection of model combinations (GHM and GCM) was made by comparing model results with observed discharge in the control period (1971–2001). Selected model combinations differed per river basin and included both different GCMs and different GHMs. This highlights the importance of using multiple hydrological models as well as multiple climate models. Models showed large differences in absolute discharge values compared to observations, so model improvement is still an important step for impact studies as well. GHMs use different model structures and parameters and will not all perform uniformly across the globe. In this study, the selection of model combinations was based on a single criterion as a first step towards a set of criteria that will reduce the range of projected changes in hydrological drought. The selected model combinations based upon the single criterion were evaluated against observations in the period 2001–2010 (the near future with respect to the control period) and model combinations showed a fairly consistent performance across the control period and the evaluation period. More research is needed both to find the best set of criteria and to improve the models, to reduce the uncertainty in projections, which is important to derive adequate adaptation measures.

With the selected model combinations (GHM and GCM), different effects of climate change on low flows were found in the river basins across the world. River basins in arid regions were projected to become even drier. In cold regions, a shift of the snow melt peak and an increase in low discharges was found. For most rivers in humid and temperate climates, model combinations gave uncertain results. Overall, results corresponded with previous studies on the effects of climate change on discharge. The change in low discharge was not everywhere equal to the change in precipitation, because discharge, of course, is affected by other processes as well (e.g. evapotranspiration) and catchment characteristics. This emphasizes the importance of the use of multiple hydrological models in climate change studies.

Besides the changes in low flows, also changes in hydrological drought characteristics (mean duration and standardized deficit volume) were determined. The drought characteristics showed an increase in most river basins, which means impacts and severity of droughts will increase as well. The increase in characteristics was not always consistent with the changes in low flows. Partly, this can be caused by the drought identification method. In case of a regime shift, unintended drought events in terms of expected impacts were identified with the threshold level method. However, drought characteristics add information about changes in drought impacts. For example, model combinations did not project a clear increase or decrease in low flows for river basins in the Amazon region, while model agreement on the amplification in drought characteristics was much larger. Given the large societal and environmental impacts of hydrological drought events, it is important to progress with finding the best drought identification method for future hydrological drought to anticipate on possible drought impacts.

Acknowledgements

The authors want to thank Nathalie Bertrand (Laboratoire de Météorologie Dynamique, France), Douglas Clark (Centre for Ecology and Hydrology, United Kingdom), Jens Heinke (Potsdam Institute for Climate Impact Research, Germany), Tobias Stacke (Max Planck Institute for Meteorology, Germany) and Frank Voss (University of Kassel, Germany) for supplying the results of the large-scale models. We wish to acknowledge all researchers involved in providing the downscaled and bias-corrected forcing data. The authors also want to thank the Global Runoff Data Centre (56068 Koblenz, Germany) for providing the observed discharge data. We also thank the two anonymous reviewers for their constructive comments. This research has partly been financially supported by the EU-FP6 Project WATCH (036946) and the EU-FP7 Project DROUGHT-R&SPI (282769). This research supports the work of the UNESCO-IHP VII EURO-FRIEND programme.

References

Alcamo, J., Döll, P., Henrichs, T., Kaspar, F., Lehner, B., Rösch, T., Siebert, S., 2003. Development and testing of the WaterGAP 2 global model of water use and availability. Hydrol. Sci. J. 48 (3), 317–337. http://dx.doi.org/10.1623/hysj.48.3.317.45290.

Arnell, N.W., 1999. Climate change and global water resources. Glob. Environ. Chang. Supplement 1 (0), , S31–S49. http://dx.doi.org/10.1016/S0959-3780(99)00017-5.

Arnell, N.W., 2003. Effects of IPCC SRES* emissions scenarios on river runoff: a global perspective. Hydrol. Earth Syst. Sci. 7 (5), 619–641. http://dx.doi.org/10.5194/hess-7-619-2003.

Arnell, N.W., Gosling, S.N., 2013. The impacts of climate change on river flow regimes at the global scale. J. Hydrol. 486 (0), 351–364. http://dx.doi.org/10.1016/j.jhydrol.2013.02.010.

Arora, V.K., Boer, G.J., 2001. Effects of simulated climate change on the hydrology of major river basins. J. Geophys. Res. Atmos. 106 (D4), 3335–3348. http://dx.doi.org/10.1029/2000JD900620.

Bates, B.C., Kundzewicz, Z.W., Wu, S., Palutikof, J.P. (Eds.), 2008. Climate Change and Water. Technical Paper of the Intergovernmental Panel on Climate Change, Intergovernmental Panel on Climate Change, Geneva.

Best, M.J., Pryor, M., Clark, D.B., Rooney, G.G., Essery, R.L.H., Ménard, C.B., Edwards, J.M., Hendry, M.A., Porson, A., Gedney, N., Mercado, L.M., Sitch, S., Blyth, E., Boucher, O., Cox, P.M., Grimmond, C.S.B., Harding, R.J., 2011. The joint UK land environment simulator (JULES), model description – Part 1: energy and water fluxes. Geosci. Model Dev. 4 (3), 677–699. http://dx.doi.org/10.5194/gmd-4-677-2011.

Bondeau, A., Smith, P.C., Zaehle, S., Schaphoff, S., Lucht, W., Cramer, W., Gerten, D., 2007. Modelling the role of agriculture for the 20th century global terrestrial carbon balance. Glob. Change Biol. 13 (3), 679–706. http://dx.doi.org/10.1111/j.1365-2486.2006.01305.x.

Chen, C., Haerter, J.O., Hagemann, S., Piani, C., 2011. On the contribution of statistical bias correction to the uncertainty in the projected hydrological cycle. Geophys. Res. Lett. 38 (20), L20403. http://dx.doi.org/10.1029/2011GL049318.

Clark, D.B., Mercado, L.M., Sitch, S., Jones, C.D., Gedney, N., Best, M.J., Pryor, M., Rooney, G.G., Essery, R.L.H., Blyth, E., Boucher, O., Harding, R.J., Huntingford, C., Cox, P.M., 2011. The joint UK land environment simulator (JULES), model description – Part 2: Carbon fluxes and vegetation dynamics. Geosci. Model Dev. 4 (3), 701–722. http://dx.doi.org/10.5194/gmd-4-701-2011.

Dai, A., 2011. Drought under global warming: a review. WIREs Clim. Change 2 (1), 45–65. http://dx.doi.org/10.1002/wcc.81.

Dai, A., 2013. Increasing drought under global warming in observations and models. Nature Clim. Change 3 (1), 52–58. http://dx.doi.org/10.1038/nclimate1633.

De Rosnay, P., Polcher, J., 1998. Modelling root water uptake in a complex land surface scheme coupled to a GCM. Hydrol. Earth Syst. Sci. 2 (2–3), 239–255. http://dx.doi.org/10.5194/hess-2-239-1998.

De Wit, M.J.M., Van Den Hurk, B., Warmerdam, P.M.M., Torfs, P.J.J.F., Roulin, E., Van Deursen, W.P.A., 2007. Impact of climate change on low-flows in the river Meuse. Clim. Chang. 82 (3–4), 351–372. http://dx.doi.org/10.1007/s10584-006-9195-2.

Duan, Q., Ajami, N.K., Gao, X., Sorooshian, S., 2007. Multi-model ensemble hydrologic prediction using Bayesian model averaging. Adv. Water Resour. 30 (5), 1371–1386. http://dx.doi.org/10.1016/j.advwatres.2006.11.014.

Feyen, L., Dankers, R., 2009. Impact of global warming on streamflow drought in Europe. J. Geophys. Res. Atmos. 114, 17. http://dx.doi.org/10.1029/2008JD011438.

Fichefet, T., Morales Maqueda, M.A., 1997. Sensitivity of a global sea ice model to the treatment of ice thermodynamics and dynamics. J. Geophys. Res. Oceans 102 (C6), 12609–12646. http://dx.doi.org/10.1029/97JC00480.

Field, C.B., Jackson, R.B., Mooney, H.A., 1995. Stomatal responses to increased CO_2: implications from the plant to the global scale. Plant Cell Environ. 18 (10), 1214–1225. http://dx.doi.org/10.1111/j.1365-3040.1995.tb00630.x.

Goosse, H., Fichefet, T., 1999. Importance of ice-ocean interactions for the global ocean circulation: a model study. J. Geophys. Res. Oceans 104 (C10), 23337–23355. http://dx.doi.org/10.1029/1999JC900215.

Gosling, S.N., Taylor, R.G., Arnell, N.W., Todd, M.C., 2011. A comparative analysis of projected impacts of climate change on river runoff from global and catchment-scale hydrological models. Hydrol. Earth Syst. Sci. 15 (1), 279–294. http://dx.doi.org/10.5194/hess-15-279-2011.

GRDC, 2013. Global Runoff Data Centre, 56068 Koblenz, Germany. <http://www.bafg.de/GRDC>.

Gudmundsson, L., Wagener, T., Tallaksen, L.M., Engeland, K., 2012. Evaluation of nine large-scale hydrological models with respect to the seasonal runoff climatology in Europe. Water Resour. Res. 48. http://dx.doi.org/10.1029/2011WR010911.

Haddeland, I., Clark, D.B., Franssen, W., Ludwig, F., Voss, F., Arnell, N.W., Bertrand, N., Best, M., Folwell, S., Gerten, D., Gomes, S., Gosling, S.N., Hagemann, S., Hanasaki, N., Harding, R., Heinke, J., Kabat, P., Koirala, S., Oki, T., Polcher, J., Stacke, T., Viterbo, P., Weedon, G.P., Yeh, P., 2011. Multi-model estimate of the global terrestrial water balance: setup and first results. J. Hydrometeorol. 12 (5), 869–884. http://dx.doi.org/10.1175/2011JHM1324.1.

Haerter, J.O., Hagemann, S., Moseley, C., Piani, C., 2011. Climate model bias correction and the role of timescales. Hydrol. Earth Syst. Sci. 15 (3), 1065–1079. http://dx.doi.org/10.5194/hess-15-1065-2011.

Hagemann, S., Dümenil, L., 1998. A parametrization of the lateral waterflow for the global scale. Clim. Dyn. 14 (1), 17–31. http://dx.doi.org/10.1007/s003820050205.

Hagemann, S., Gates, L.D., 2003. Improving a subgrid runoff parameterization scheme for climate models by the use of high resolution data derived from satellite observations. Clim. Dyn. 21 (3–4), 349–359. http://dx.doi.org/10.1007/s00382-003-0349-x.

Hagemann, S., Chen, C., Haerter, J.O., Heinke, J., Gerten, D., Piani, C., 2011. Impact of a statistical bias correction on the projected hydrological changes obtained from three GCMs and two hydrology models. J. Hydrometeorol. 12 (4), 556–578. http://dx.doi.org/10.1175/2011JHM1336.1.

Hagemann, S., Chen, C., Clark, D.B., Folwell, S., Gosling, S.N., Haddeland, I., Hanasaki, N., Heinke, J., Ludwig, F., Voss, F., Wiltshire, A.J., 2013. Climate change impact on available water resources obtained using multiple global climate and hydrology models. Earth Syst. Dyn. 4 (1), 129–144. http://dx.doi.org/10.5194/esd-4-129-2013.

Hall, A., Qu, X., 2006. Using the current seasonal cycle to constrain snow albedo feedback in future climate change. Geophys. Res. Lett. 33, L03502. http://dx.doi.org/10.1029/2005GL025127.

Hirabayashi, Y., Kanae, S., Emori, S., Oki, T., Kimoto, M., 2008. Global projections of changing risks of floods and droughts in a changing climate. Hydrol. Sci. J. 53 (4), 754–772. http://dx.doi.org/10.1623/hysj.53.4.754.

Hisdal, H., Tallaksen, L.M., Clausen, B., Peters, E., Gustard, A., 2004. Hydrological drought characteristics. In: Tallaksen, L.M., van Lanen, H.A.J. (Eds.), Hydrological Drought Processes and Estimation Methods for Streamflow and Groundwater. Elsevier Science B.V., Developments in Water Science, vol. 48, pp. 139–198.

Hourdin, F., Musat, I., Bony, S., Braconnot, P., Codron, F., Dufresne, J.-L., Fairhead, L., Filiberti, M.-A., Friedlingstein, P., Grandpeix, J.-Y., Krinner, G., LeVan, P., Li, Z.-X., Lott, F., 2006. The LMDZ4 general circulation model: climate performance and sensitivity to parametrized physics with emphasis on tropical convection. Clim. Dyn. 27 (7–8), 787–813. http://dx.doi.org/10.1007/s00382-006-0158-0.

Huntington, T.G., 2008. CO_2-induced suppression of transpiration cannot explain increasing runoff. Hydrol. Process. 22 (2), 311–314. http://dx.doi.org/10.1002/hyp.6925.

Johnson, F., Westra, S., Sharma, A., Pitman, A.J., 2011. An assessment of GCM skill in simulating persistence across multiple time scales. J. Clim. 24 (14), 3609–3623. http://dx.doi.org/10.1175/2011JCLI3732.1.

Jungclaus, J.H., Keenlyside, N., Botzet, M., Haak, H., Luo, J.-J., Latif, M., Marotzke, J., Mikolajewicz, U., Roeckner, E., 2006. Ocean circulation and tropical variability in the coupled model ECHAM5/MPI-OM. J. Clim. 19 (16), 3952–3972. http://dx.doi.org/10.1175/JCLI3827.1.

Lammertsma, E.I., de Boer, H.J., Dekker, S.C., Dilcher, D.L., Lotter, A.F., Wagner-Cremer, F., 2011. Global CO_2 rise leads to reduced maximum stomatal conductance in Florida vegetation. Proc. Natl. Acad. Sci. USA 108 (10), 4035–4040. http://dx.doi.org/10.1073/pnas.1100371108.

Madadgar, S., Moradkhani, H., 2013. Drought analysis under climate change using copula. J. Hydrol. Eng. 18 (7), 746–759. http://dx.doi.org/10.1061/(ASCE)HE.1943-5584.0000532.

Manabe, S., Milly, P.C.D., Wetherald, R., 2004. Simulated long-term changes in river discharge and soil moisture due to global warming. Hydrol. Sci. J. 49 (4). http://dx.doi.org/10.1623/hysj.49.4.625.54429.

Masson, D., Knutti, R., 2011. Climate model genealogy. Geophys. Res. Lett. 38 (8), L08703. http://dx.doi.org/10.1029/2011GL046864.

Milly, P.C.D., Dunne, K.A., Vecchia, A.V., 2005. Global pattern of trends in streamflow and water availability in a changing climate. Nature 438 (7066), 347–350. http://dx.doi.org/10.1038/nature04312.

Mishra, A.K., Singh, V.P., 2010. A review of drought concepts. J. Hydrol. 391, 202–216. http://dx.doi.org/10.1016/j.jhydrol.2010.07.012.

Najafi, M.R., Moradkhani, H., Jung, I.W., 2011. Assessing the uncertainties of hydrologic model selection in climate change impact studies. Hydrol. Process. 25 (18), 2814–2826. http://dx.doi.org/10.1002/hyp.8043.

Nakićenović, N., Swart, R., 2000. Special Report on Emissions Scenarios: A Special Report of Working Group III of the Intergovernmental Panel on Climate Change. Tech. Rep., Cambridge University Press.

Nash, J.E., Sutcliffe, J.V., 1970. River flow forecasting through conceptual models Part I – a discussion of principles. J. Hydrol. 10 (3), 282–290. http://dx.doi.org/10.1016/0022-1694(70)90255-6.

Nijssen, B., O'Donnell, G.M., Hamlet, A., Lettenmaier, D., 2001a. Hydrologic sensitivity of global rivers to climate change. Clim. Change 50 (1–2), 143–175. http://dx.doi.org/10.1023/A:1010616428763.

Nijssen, B., O'Donnell, G.M., Lettenmaier, D.P., Lohmann, D., Wood, E.F., 2001b. Predicting the discharge of global rivers. J. Clim. 14 (15), 3307–3323, doi:10.1175/1520-0442(2001)014<3307:PTDOGR>2.0.CO;2.

Nohara, D., Kitoh, A., Hosaka, M., Oki, T., 2006. Impact of climate change on river discharge projected by multimodel ensemble. J. Hydrometeorol. 7 (5), 1076–1089. http://dx.doi.org/10.1175/JHM531.1.

Orlowsky, B., Seneviratne, S.I., 2013. Elusive drought: uncertainty in observed trends and short- and long-term CMIP5 projections. Hydrol. Earth Syst. Sci. 17 (5), 1765–1781. http://dx.doi.org/10.5194/hess-17-1765-2013.

Parrish, M.A., Moradkhani, H., DeChant, C.M., 2012. Toward reduction of model uncertainty: integration of Bayesian model averaging and data assimilation. Water Resour. Res. 48 (3), W03519. http://dx.doi.org/10.1029/2011WR011116.

Peel, M.C., Finlayson, B.L., McMahon, T.A., 2007. Updated world Köppen–Geiger climate classification map. Hydrol. Earth Syst. Sci. 11, 1633–1644. http://dx.doi.org/10.5194/hess-11-1633-2007.

Piani, C., Weedon, G., Best, M., Gomes, S., Viterbo, P., Hagemann, S., Haerter, J., 2010. Statistical bias correction of global simulated daily precipitation and temperature for the application of hydrological models. J. Hydrol. 395, 199–215. http://dx.doi.org/10.1016/j.jhydrol.2010.10.024.

Prudhomme, C., Giuntoli, I., Robinson, E.L., Clark, D.B., Arnell, N.W., Dankers, R., Fekete, B.M., Franssen, W., Gerten, D., Gosling, S.N., Hagemann, S., Hannah, D.M., Kim, H., Masaki, Y., Satoh, Y., Stacke, T., Wada, Y., Wisser, D., 2013. Hydrological droughts in the 21st century, hotspots and uncertainties from a global multimodel ensemble experiment. Proc. Natl. Acad. Sci. USA. http://dx.doi.org/10.1073/pnas.1222473110 (published ahead of print December 16, 2013).

Reifen, C., Toumi, R., 2009. Climate projections: past performance no guarantee of future skill? Geophys. Res. Lett. 36 (13). http://dx.doi.org/10.1029/2009GL038082.

Romm, J., 2011. The next dust bowl. Nature 478, 450–451. http://dx.doi.org/10.1038/478450a.

Rost, S., Gerten, D., Bondeau, A., Lucht, W., Rohwer, J., Schaphoff, S., 2008. Agricultural green and blue water consumption and its influence on the global water system. Water Resour. Res. 44 (9), 1–12. http://dx.doi.org/10.1029/2007WR006331.

Royer, J.-F., Cariolle, D., Chauvin, F., Déqué, M., Douville, H., Hu, R.-M., Planton, S., Rascol, A., Ricard, J.-L., Melia, D.S.Y., Sevault, F., Simon, P., Somot, S., Tyteca, S., Terray, L., Valcke, S., 2002. Simulation des changements climatiques au cours du XXIe siècle incluant l'ozone stratosphérique. CR Geosci. 334 (3), 147–154. http://dx.doi.org/10.1016/S1631-0713(02)01728-5.

Salas Mélia, D., 2002. A global coupled sea ice-ocean model. Ocean Modell. 4 (2), 137–172. http://dx.doi.org/10.1016/S1463-5003(01)00015-4.

Seneviratne, S.I., Nicholls, N., Easterling, D., Goodess, C.M., Kanae, S., Kossin, J., Luo, Y., Marengo, J., McInnes, K., Rahimi, M., Reichstein, M., Sorteberg, A., Vera, C., Zhang, X., 2012. Changes in climate extremes and their impacts on the natural physical environment. In: Field, C.B., Barros, V., Stocker, T.F., Qin, D., Dokken, D.J., Ebi, K.L., Mastrandrea, M.D., Mach, K.J., Plattner, G.K., Allen, S.K., Tignor, M., Midgley, P.M. (Eds.), Managing the Risks of Extreme Events and Disasters to Advance Climate Change Adaptation, A Special Report of Working Groups I and II of the Intergovernmental Panel on Climate Change. Cambridge University Press, Cambridge, UK, and New York, NY, USA, pp. 109–230.

Sheffield, J., Wood, E.F., 2008. Projected changes in drought occurrence under future global warming from multi-model, multi-scenario, IPCC AR4 simulations. Clim. Dyn. 31 (1), 79–105. http://dx.doi.org/10.1007/s00382-007-0340-z.

Sperna Weiland, F.C., van Beek, L.P.H., Kwadijk, J.C.J., Bierkens, M.F.P., 2010. The ability of a GCM-forced hydrological model to reproduce global discharge variability. Hydrol. Earth Syst. Sci. 14 (8), 1595–1621. http://dx.doi.org/10.5194/hess-14-1595-2010.

Sperna Weiland, F.C., van Beek, L.P.H., Kwadijk, J.C.J., Bierkens, M.F.P., 2012. Global patterns of change in discharge regimes for 2100. Hydrol. Earth Syst. Sci. 16 (4), 1047–1062. http://dx.doi.org/10.5194/hess-16-1047-2012.

Stegehuis, A.I., Teuling, A.J., Ciais, P., Vautard, R., Jung, M., 2013. Future European temperature change uncertainties reduced by using land heat flux observations. Geophys. Res. Lett. 40 (10), 2242–2245. http://dx.doi.org/10.1002/grl.50404.

Tallaksen, L.M., van Lanen, H.A.J. (Eds.), 2004. Hydrological Drought: Processes and Estimation Methods for Streamflow and Groundwater. Elsevier Science BV, Developments in Water Science, vol. 48. The Netherlands.

Tang, Q., Lettenmaier, D.P., 2012. 21st century runoff sensitivities of major global river basins. Geophys. Res. Lett. 39 (6). http://dx.doi.org/10.1029/2011GL050834.

Van Huijgevoort, M.H.J., Hazenberg, P., van Lanen, H.A.J., Teuling, A.J., Clark, D.B., Folwell, S., Gosling, S.N., Hanasaki, N., Heinke, J., Koirala, S., Stacke, T., Voss, F., Sheffield, J., Uijlenhoet, R., 2013. Global multi-model analysis of drought in runoff for the second half of the 20th century. J. Hydrometeorol. 14 (5), 1535–1552. http://dx.doi.org/10.1175/JHM-D-12-0186.1.

Van Lanen, H.A.J., Wanders, N., Tallaksen, L.M., Van Loon, A.F., 2013. Hydrological drought across the world: impact of climate and physical catchment structure. Hydrol. Earth Syst. Sci. 17 (5), 1715–1732. http://dx.doi.org/10.5194/hess-17-1715-2013.

Van Loon, A.F., Van Lanen, H.A.J., 2012. A process-based typology of hydrological drought. Hydrol. Earth Syst. Sci. 16 (7), 1915–1946. http://dx.doi.org/10.5194/hess-16-1915-2012.

Vidal, J.-P., Martin, E., Kitova, N., Najac, J., Soubeyroux, J.-M., 2012. Evolution of spatio-temporal drought characteristics: validation, projections and effect of adaptation scenarios. Hydrol. Earth Syst. Sci. 16 (8), 2935–2955. http://dx.doi.org/10.5194/hess-16-2935-2012.

Wanders, N., van Lanen, H.A.J., van Loon, A.F., 2010. Indicators for Drought Characterization on a Global Scale. WATCH Technical Report 24. <http://www.eu-watch.org/publications/technical-reports> (accessed on 09.08.13).

Weedon, G.P., Gomes, S., Viterbo, P., Shuttleworth, W.J., Blyth, E., Österle, H., Adam, J.C., Bellouin, N., Boucher, O., Best, M., 2011. Creation of the WATCH forcing data and its use to assess global and regional reference crop evaporation over land during the twentieth century. J. Hydrometeorol. 12 (5), 823–848. http://dx.doi.org/10.1175/2011JHM1369.1.

in Wilhite, D. (Ed.), 2000. DROUGHT A Global Assessment. Routledge Hazards and Disasters Series, vol I &II. Routledge, London.

Yevjevich, V., 1967. An Objective Approach to Definition and Investigations of Continental Hydrologic Droughts. Hydrology Papers 23. Colorado State University, Fort Collins, USA.